Supplementary materials for Bridging wastewater and case surveillance reveals the hidden burden of the 2022 mpox outbreak

February 2, 2026

Caroline Mburu[1,2,*], Aidan M. Nikiforuk[2,13],Ana Citlali Marquez[3], Agatha N. Jassem[3], Natalie Prystajecky[3], Chloe G. Xavier[4], Katherine A. Twohig[4,14], Venessa Ryan[4], Kirsty Bobrow[4], Natalie C. Knox[6,7], Chand S. Mangat[6,7], Mark Gilbert[4,12], Mathieu Maheu-Giroux[5], Sharmistha Mishra[8,9,10,11], Hind Sbihi[2,12], Michael A. Irvine[1,2,13]

[1] Faculty of Health Sciences, Simon Fraser University, Burnaby, British Columbia, Canada

[2] Data Science & Innovation, British Columbia Centre for Disease Control, Vancouver, British Columbia, Canada

[3] Public Health Laboratory, British Columbia Centre for Disease Control, Vancouver, British Columbia, Canada

[4] Clinical and prevention services, British Columbia Centre for Disease Control, Vancouver, British Columbia, Canada

[5] Department of Epidemiology and Biostatistics, School of Population and Global Health, McGill University, Montréal, Québec, Canada

[6] National Microbiology Laboratory, Public Health Agency of Canada, Winnipeg, Manitoba, Canada

[7] Department of Medical Microbiology and Infectious Diseases, University of Manitoba, Winnipeg, Manitoba, Canada

[8] MAP Centre for Urban Health Solutions, Unity Health Toronto, Toronto, Ontario, Canada

[9] Institute of Medical Sciences, University of Toronto, Toronto, Ontario, Canada

[10] Department of Medicine, St. Michael's Hospital, University of Toronto, Toronto, Ontario, Canada

[11] Dalla Lana School of Public Health, University of Toronto, Toronto, Ontario, Canada

[12] School of Population and Public Health, University of British Columbia, Vancouver, British Columbia, Canada

[13] Department of Statistics, University of British Columbia, Vancouver, British Columbia, Canada

[14] PHAC, Canadian Field Epidemiology Program, Public Health Agency of Canada

*Corresponding author. Email: caroline.mburu@bccdc.ca

Additional information

S1. Full Model Equations

For each sexual activity group $g \in \{1, 2, 3\}$ and vaccination status $v \in \{0, 1, 2\}$ ($v = 0$: unvaccinated, $v = 1$: one dose, $v = 2$: two doses), the compartmental dynamics are:

Susceptible:

$$\begin{aligned}
\frac{dS_{0,g}}{dt} &= -\lambda_g(t)S_{0,g}(t) - \alpha_1(t)S_{0,g}(t) \\
\frac{dS_{1,g}}{dt} &= \alpha_1(t)S_{0,g}(t) - \lambda_g(t)(1 - \mathrm{ve}_1)S_{1,g}(t) - \alpha_2(t)S_{1,g}(t) \\
\frac{dS_{2,g}}{dt} &= \alpha_2(t)S_{1,g}(t) - \lambda_g(t)(1 - \mathrm{ve}_2)S_{2,g}(t)
\end{aligned}$$

Exposed:

$$\frac{dE_{v,g}}{dt} = \lambda_g(t)(1 - \mathrm{ve}_v)S_{v,g}(t) - \epsilon_v E_{v,g}(t)$$

Presymptomatic:

$$\frac{dP_{v,g}}{dt} = \epsilon_v E_{v,g}(t) - \omega_v P_{v,g}(t)$$

Asymptomatic (3-stage Gamma):

$$\begin{aligned}
\frac{dA^1_{v,g}}{dt} &= m\,\omega_v P_{v,g}(t) - 3\theta_v A^1_{v,g}(t) \\
\frac{dA^2_{v,g}}{dt} &= 3\theta_v A^1_{v,g}(t) - 3\theta_v A^2_{v,g}(t) \\
\frac{dA^3_{v,g}}{dt} &= 3\theta_v A^2_{v,g}(t) - 3\theta_v A^3_{v,g}(t)
\end{aligned}$$

Symptomatic (3-stage Gamma):

$$\begin{aligned}
\frac{dI^1_{v,g}}{dt} &= (1 - m)\,\omega_v P_{v,g}(t) - 3\gamma_v I^1_{v,g}(t) \\
\frac{dI^2_{v,g}}{dt} &= 3\gamma_v I^1_{v,g}(t) - 3\gamma_v I^2_{v,g}(t) \\
\frac{dI^3_{v,g}}{dt} &= 3\gamma_v I^2_{v,g}(t) - 3\gamma_v I^3_{v,g}(t)
\end{aligned}$$

Recovered:

$$\frac{dR_g}{dt} = \sum_{v=0}^{2} \left(3\theta_v A^3_{v,g}(t) + 3\gamma_v I^3_{v,g}(t)\right)$$

Force of Infection

We considered a single transmission pathway for mpox; transmission through close contact during sexual partnerships among gbMSM individuals. The *force of infection*, $\lambda_g(t)$, represents

the per capita rate of mpox acquisition for individuals in sexual activity group g at time t. It is defined as:

$$\lambda_g(t) = \beta \cdot c_g \cdot \sum_{g'=1}^{3} M_{g,g'}(t) \cdot \text{prev}_{g'}(t), \tag{1}$$

where β is the probability of transmission per effective contact, c_g is the average number of sexual contacts per person per day in group g, $M_{g,g'}(t)$ is the time-varying sexual mixing matrix representing the probability that a contact made by an individual in group g is with an individual in group g', $\text{prev}_{g'}(t)$ is the prevalence of infectious individuals in group g' at time t. The transmission probability per effective contact, β, was estimated within the model using a truncated normal prior:

$$\beta \sim \text{N}_{[0,1]}(\mu = 0.8, \sigma = 0.1).$$

This prior reflects evidence from previous modeling studies that reported relatively high transmission probabilities for mpox among gbMSM populations during the 2022 outbreak [1]. The mean of 0.8 was chosen to represent a biologically plausible upper-bound scenario, while the standard deviation of 0.1 allows for moderate uncertainty. Truncation ensures the parameter remains within the valid probability interval $[0, 1]$.

Mixing Matrix

The sexual mixing matrix $M_{g,g'}(t)$ incorporates both assortative and proportional mixing by sexual activity groups, governed by a mixing parameter κ. This parameter governs the degree to which individuals preferentially mix within their own group versus proportionally across groups. We modeled κ using a Beta prior distribution

$$\kappa \sim \text{Beta}(40, 2),$$

which favours higher probabilities of within group mixing . The mixing matrix is defined as;

$$M_{g,g'}(t) = \kappa \cdot \delta_{g,g'} + (1 - \kappa) \cdot \frac{c_{g'} \cdot N_{g'}}{\sum_{g''} c_{g''} \cdot N_{g''}}, \tag{2}$$

where $\delta_{g,g'}$ is the Kronecker delta (1 if $g = g'$, 0 otherwise) and N_g is the population size of group g [1].

Prevalence of Infectious Individuals

The prevalence of infectious individuals in group g at time t, $\text{prev}_g(t)$, includes individuals who are symptomatically infectious (I), asymptomatically infectious (A), and presymptomatically infectious (P) across all vaccination statuses. Contributions from A and P compartments to the force of infection are adjusted by their relative infectiousness compared to symptomatically infectious (I) using the factor ρ=0.776 [2]

$$\text{prev}_g(t) = \frac{1}{N_g}\Bigg[\rho\Big(P_g^u(t) + P_g^{va}(t) + P_g^{vb}(t)\Big) + \rho\sum_{i=1}^{3}\Big(A_{i,g}^u(t) + A_{i,g}^{va}(t) + A_{i,g}^{vb}(t)\Big) + \sum_{i=1}^{3}\Big(I_{i,g}^u(t) + I_{i,g}^{va}(t) + I_{i,g}^{vb}(t)\Big)\Bigg]. \tag{3}$$

S2. Wastewater viral load

Deposited Viral Load in Wastewater

The daily concentration of MPXV DNA deposited into the wastewater was calculated based on the number of individuals actively shedding virus. All infectious individuals i.e. presymptomatic (P), asymptomatic (A), and symptomatic (I) including vaccinated individuals were assumed to contribute to viral shedding. In the absence of robust empirical data quantifying differences in stage-specific viral shedding conditional on vaccination status for mpox, baseline analyses assumed equal shedding rates for vaccinated and unvaccinated individuals once infected. Potential post-infection effects of vaccination on viral shedding were explored through sensitivity analyses rather than imposed in the baseline model. Although individuals in the exposed compartment (E) may begin shedding prior to becoming infectious, they were assumed not to contribute significantly to viral shedding.

We derived viral shedding rates using data from a previous study [3] which investigated viral dynamics in individuals with confirmed mpox infection in Spain. The study quantified viral DNA loads at multiple anatomical sites including skin lesions, rectum, saliva, semen, and blood over time using qPCR. We focused on rectal and skin lesion viral load data, given their potential relevance to fecal shedding and contact with wastewater systems. The study provided median viral DNA concentrations (in $\log_{10}$ copies/mL) at symptom onset and estimated median clearance times for each anatomical site. To extract detailed shedding dynamics over time, we digitized the probability of detectable virus over days since symptom onset using the juicr R package [4]. For each anatomical site, we aligned the baseline probability (1.0) with the reported median viral load at day 0, and extracted relative load values for subsequent days. We computed shedding estimates corresponding to the midpoint of each of the three infectious stages. We then summed the values from skin and rectal shedding and used these as the viral shedding rates (ϕ_i) for the three symptomatic stages I_1, I_2, and I_3,

$$\phi_i = \{12.3,\ 11.5,\ 10.2\}\ \log_{10}\ \text{copies/mL}.$$

For presymptomatic and asymptomatic individuals, we assumed reduced viral shedding relative to symptomatic individuals. We used a multiplicative factor ρ =0.776 [2] representing the infectiousness and fecal shedding of presymptomatic and asymptomatic individuals relative to symptomatic individuals. The total deposited viral load $V_{\text{shed}}(t)$ at time t was defined as:

$$V_{\text{shed}}(t) = \psi \cdot \rho \sum_{i=1}^{n} \phi_i P_i(t) + \sum_{i=1}^{n} \phi_i I_i(t) + \rho \sum_{i=1}^{n} \phi_i A_i(t)$$

,

where ϕ_i is the viral shedding rate associated with compartment i, ρ is the relative reduction in viral shedding for presymptomatic and asymptomatic individuals compared to symptomatic individuals and ψ is a scaling parameter accounting for uncertainty in total wastewater viral load estimates. We fitted the scaling parameter ψ using a lognormal distribution prior to account for uncertainty in the mapping between model-predicted viral shedding and observed concentrations in wastewater. The prior was specified as:

$$\psi \sim \text{LogNormal}\big(\log(3 \times 10^{-9}),\, 0.158\big).$$

This prior reflects prior knowledge that the scaling factor is expected to be small and positive, while allowing for uncertainty due to variability in viral decay, sampling efficiency, and transport dynamics within the sewer system.

Transport and Sampled Viral Load

To simulate the delay and degradation of MPXV viral DNA from the point of shedding to the point of sampling, we employed a simplified advection-dispersion-decay framework [5]. This model captures delay and decrease of signal of viral particles caused by hydrodynamic and environmental processes including dilution, sedimentation, resuspension and other factors within the sewer network. The model includes two key components; An exponential decay term with rate μ, representing first-order degradation of MPXV DNA in wastewater due to biological activity and environmental stressors and a plug-flow delay kernel $g(\tau)$, representing the distribution of transit times τ that viral particles experience between shedding and sampling.

The total sampled viral concentration $V_s(t)$ at time t is then modeled as the convolution of the deposited viral load $V_{\text{shed}}(t)$ and the delay distribution $g(\tau)$, incorporating both temporal dispersion and exponential decay:

$$V_s(t) = \int_0^t (V_{\text{shed}}(t-\tau) \cdot g(\tau) \cdot e^{-\mu\tau}\, d\tau$$

For computational efficiency, the plug-flow delay distribution $g(\tau)$ was approximated using a Gaussian distribution with mean transit time $\bar{\tau}$ and standard deviation σ allowing us to capture the average lag and its variability:

$$g(\tau) = \frac{1}{\sqrt{2\pi}\sigma} \exp\left(-\frac{(\tau-\bar{\tau})^2}{2\sigma^2}\right).$$

The mean transit time $\bar{\tau}$ and its standard deviation σ, which characterize the distribution of delays between viral shedding and sampling, were estimated within the model using weakly informative priors. These priors were chosen to reflect plausible transport dynamics for the local sewer system, while allowing the data to guide inference. Specifically, the prior for the mean transit time $\bar{\tau}$ was a truncated normal distribution centered at 2.5 days, with a standard

deviation of approximately 0.5 days,constrained to be positive

$$\tau \sim \mathrm{N}_{[0.1,10)}(2.5,\ 0.5^2).$$

The standard deviation σ of the delay distribution was assigned a truncated normal prior centered at 0.3 days, with a standard deviation of 0.1, constrained to be positive:

$$\sigma \sim \mathrm{N}_{[0.1,1)}(0.3,\ 0.1^2).$$

These choices reflect prior expectations of moderate variability in sewer travel times, based on hydrodynamic behavior, while ensuring estimates remain within realistic bounds. In contrast, the viral decay rate μ was held fixed because jointly estimating decay, transit time, and dispersion led to identifiability issues. We therefore used a fixed decay rate of $\mu = 0.143\,\mathrm{day}^{-1}$ consistent with Jacob et al [6], who measured MPXV DNA degradation in influent wastewater. Using this empirically grounded value allowed us to parameterize decay realistically while avoiding over-parameterization of the wastewater transport model.

S3. Likelihood specification and model fitting

We fitted three versions of the model: (i) a case-data-only model, (ii) a viral-load-only model, and (iii) a combined case and viral load model. All models were implemented with a daily time step and fitted within a Bayesian framework using `rjags`, which relies on Markov Chain Monte Carlo (MCMC) sampling. JAGS primarily employs Gibbs sampling, but uses adaptive Metropolis-Hastings steps within the Gibbs sampler for parameters whose full conditional distributions do not have standard forms.

Each model was run using two parallel MCMC chains with 50,000 iterations per chain. The first 10,000 iterations were discarded as burn-in to allow the chains to reach the target distribution. The remaining samples were thinned by a factor of 3 to reduce autocorrelation. Convergence was assessed through visual inspection of trace plots and the Gelman–Rubin diagnostic ($\hat{R}$), ensuring that all monitored parameters had $\hat{R} < 1.1$.

To initiate the model, we estimated initial conditions for the exposed (E), pre-symptomatic (P), asymptomatic stage 1 (A_1), and symptomatic stage 1 (I_1) compartments. Priors for the total number of individuals in each compartment at $t = 1$ were specified as:

$$\begin{aligned} E_0 &\sim \mathrm{Poisson}(3), \\ P_0 &\sim \mathrm{Poisson}(1), \\ A_{10} &\sim \mathrm{Poisson}(1), \\ I_{10} &\sim \mathrm{Poisson}(1). \end{aligned}$$

To reflect heterogeneity in exposure risk across the three behavioral groups, we normalized the daily sexual contact rate in each group (c_g):

$$w_g = \frac{c_g}{\sum_{g=1}^{3} c_g}$$

These normalized weights were used to allocate the initial state values across groups proportionally:

$$E_g(1) = E_0 \cdot w_g,$$
$$P_g(1) = P_0 \cdot w_g,$$
$$A_{1g}(1) = A_{10} \cdot w_g,$$
$$I_{1g}(1) = I_{10} \cdot w_g.$$

Initial values for other compartments were initialized to zero, with the exception of the susceptible compartments. Prior to fitting the model to data, we simulated the system forward for an initial 30-day period without data assimilation. This allowed the compartmental dynamics to stabilize and reduce sensitivity to initial value assumptions.

Case data Model

We assumed observed case counts were *negative binomially* distributed to account for overdispersion. Specifically, for each time point t, the number of reported cases C_t was modeled as:

$$C_t \sim \text{NegBin}(\widehat{C}_t, \eta),$$

where $\widehat{C}_t$ denotes the model predicted mean number of reported cases and η is the dispersion parameter. We specified a *gamma prior* for the dispersion:

$$\eta \sim \text{Gamma}(2, 0.5),$$

which has a mean of 4 and a standard deviation of approximately 2.8 reflecting moderate overdispersion. To align model-predicted infections with observed case reporting, we incorporated a reporting lag fixed at an average of 7 days. This delay was informed by the interval between symptom onset and laboratory confirmation dates in the empirical line list data. We also included a reporting fraction, rf, to account for the fact that not all symptomatic individuals are captured by the surveillance system. Underdetection, especially during the early outbreak period, has been documented in several studies. For instance, Brand et al. [2] estimated a mean weekly probability of detection of 0.45, while Xiu et al. [1] reported a detection fraction of approximately 78% (95%Crl:0.48-0.96) prior to the start of vaccination in Vancouver. Based on sensitivity analyses, we specified the prior for the reporting fraction as:

$$\text{rf} \sim \text{Beta}(10, 10),$$

corresponding to a mean of 0.50, with flexibility to accommodate substantial uncertainty. The proportion of infections that remain asymptomatic m was assigned a Beta prior informed by a recent meta-analysis estimating that 34% of infections are asymptomatic [7]:

$$m \sim \text{Beta}(6.8, 13.2)$$

We assumed that vaccine effectiveness was 66.0% (95% CI: 47.4–78.1) for individuals who

received two doses, and 35.8% (95% CI: 22.1–47.1) for those who received a single dose. These estimates were based on findings from a case-control study evaluating the effectiveness of mpox vaccine in adults [8]. Beta prior distributions were assigned to the one and two dose effectiveness parameters, denoted ve_1 and ve_2, respectively:

$$\text{ve}_1 \sim \text{Beta}(22.05, 39.56),$$
$$\text{ve}_2 \sim \text{Beta}(20.92, 10.77)$$

Finally, prior distributions for other model parameters governing transitions between compartments i.e latent and infectious periods were informed by existing literature on the biological and epidemiological characteristics of mpox. A complete summary of all prior distributions is provided in Table 1

Viral Load Model

We used the sampled viral load $V_s(t)$, previously derived from model predicted shedding and transport dynamics, as the basis for comparison to empirical wastewater viral load data. To scale and standardize the model predicted viral load, $V_s(t)$ was multiplied by the daily wastewater flow rate and divided by the population served by the sewershed, yielding daily viral load per capita in copies/mL. We then extracted values only for time points corresponding to days with available wastewater samples.

The resulting concentrations were log-transformed (base 10) to match the scale of reported data. We refer to this final model predicted log-transformed viral load as $V_r(t)$, the reported viral load. For each observed day t, the measured $\log_{10}$ viral concentration was modeled using a normal likelihood:

$$V_{\text{obs}}(t) \sim \text{Normal}\left(V_r(t), \frac{1}{\tau_{\text{ww}}}\right)$$

where $V_{\text{obs}}(t)$ is the observed log-transformed viral load on day t, $V_r(t)$ is the model-predicted reported viral load, and τ_{ww} is the precision parameter representing observational uncertainty. We assigned a Gamma prior to τ_{ww}:

$$\tau_{\text{ww}} \sim \text{Gamma}(2, 1)$$

The Gamma distribution ensures positivity while allowing data driven estimation of observation uncertainty.

Combined Model

For the combined model, we retained the same compartmental structure and equations used in the individual case-data only and viral-load only models. The combined model incorporated both data sources by jointly specifying the likelihoods for observed case counts and observed wastewater viral load. This allowed simultaneous fitting to both clinical and environmental data streams while sharing the same underlying transmission dynamics.

S4. Additional figures and tables

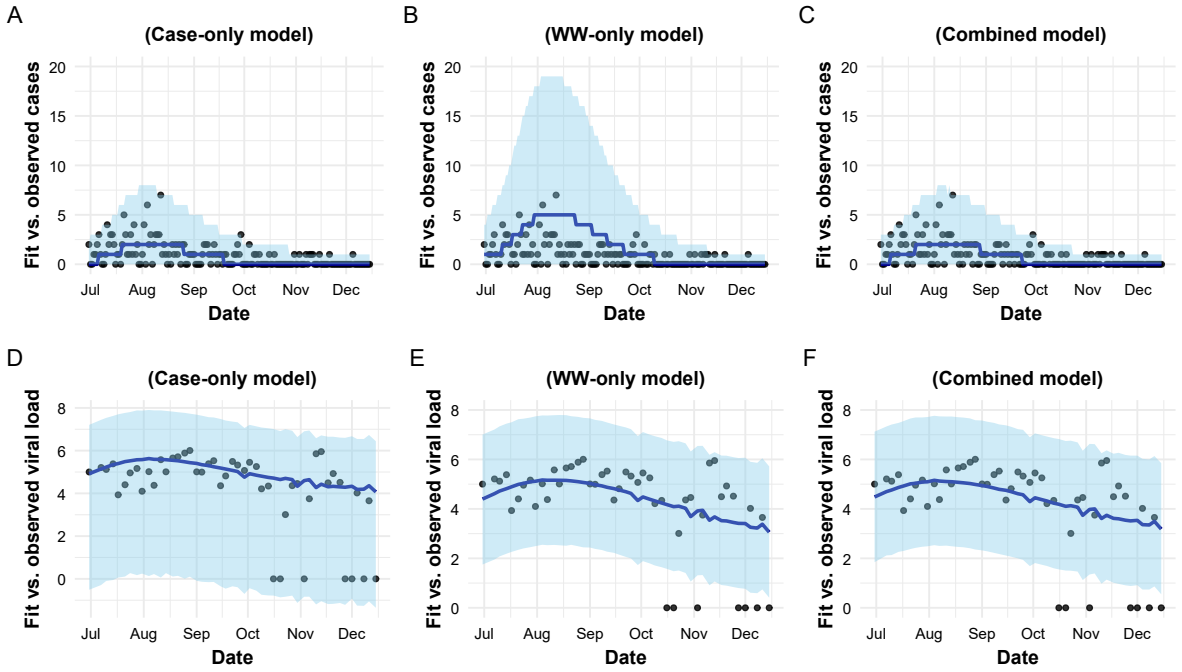

Figure S1: Posterior predictive fits of reported cases (A–C) and wastewater viral load (D–F) under the case-only, combined, and wastewater-only models. Black points represent observed data, blue lines show posterior medians, and shaded regions indicate 95% credible intervals.

Table S1: Convergence diagnostics for case-only, wastewater-only, and combined models. R-hat values (all equal to 1) indicate convergence across chains. Effective sample sizes (ESS) are > 200

	R-hat			ESS		
Parameter	Case-only	WW-only	Combined	Case-only	WW-only	Combined
$\log \psi$	1	1	1	40000	10031	18325
$\bar{\tau}$	1	1	1	40312	9402	17352
σ	1	1	1	40000	16057	31819
τ_{ww}	1	1	1	40000	38857	77552
β	1	1	1	15845	23556	27434
κ	1	1	1	14378	13093	30214
rf	1	1	1	11027	40000	24049
ϕ_i	1	1	1	19823	40000	43526
δ	1	1	1	30084	34298	54837
θ	1	1	1	19543	25799	37937
ω	1	1	1	30463	33256	53995
ve_1	1	1	1	33907	34550	68146
ve_2	1	1	1	35439	35654	71169
m	1	1	1	19493	34523	41743

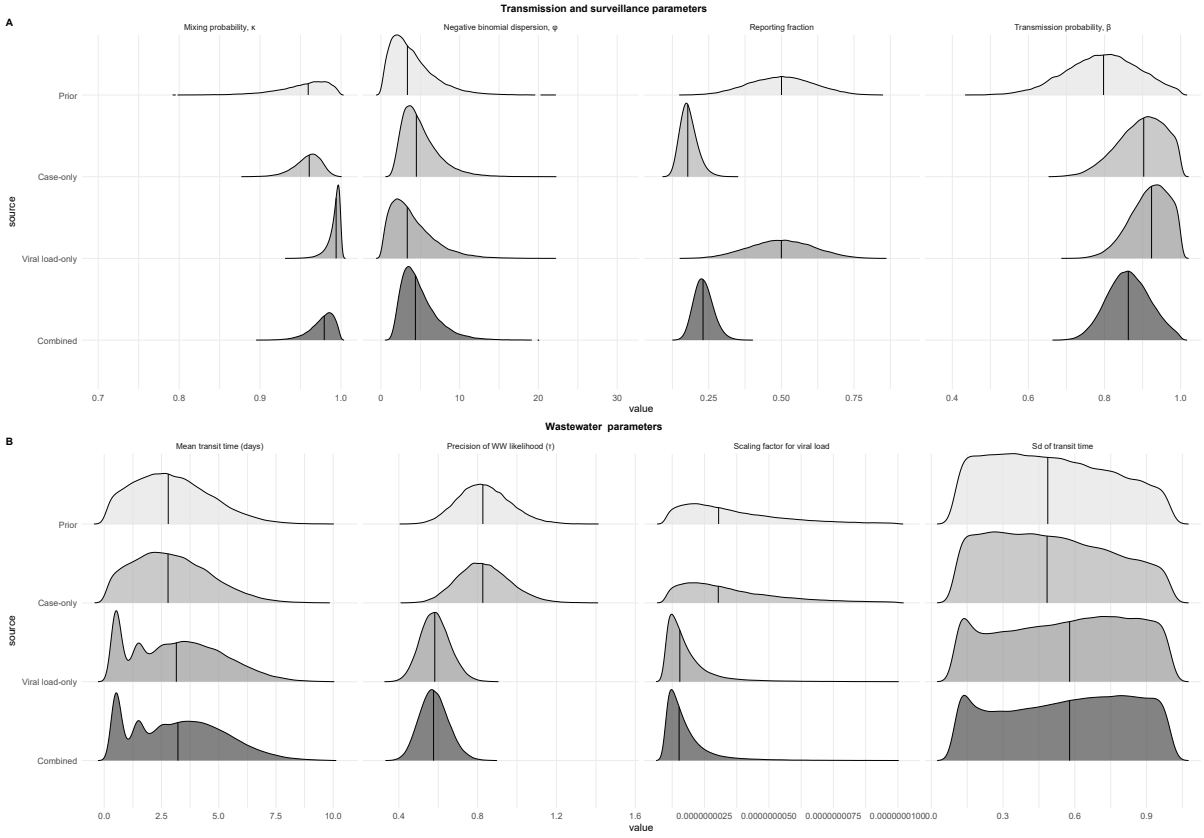

Figure S2: Posterior and prior distributions of key transmission, surveillance, and wastewater parameters across case-only, wastewater-only, and combined models.

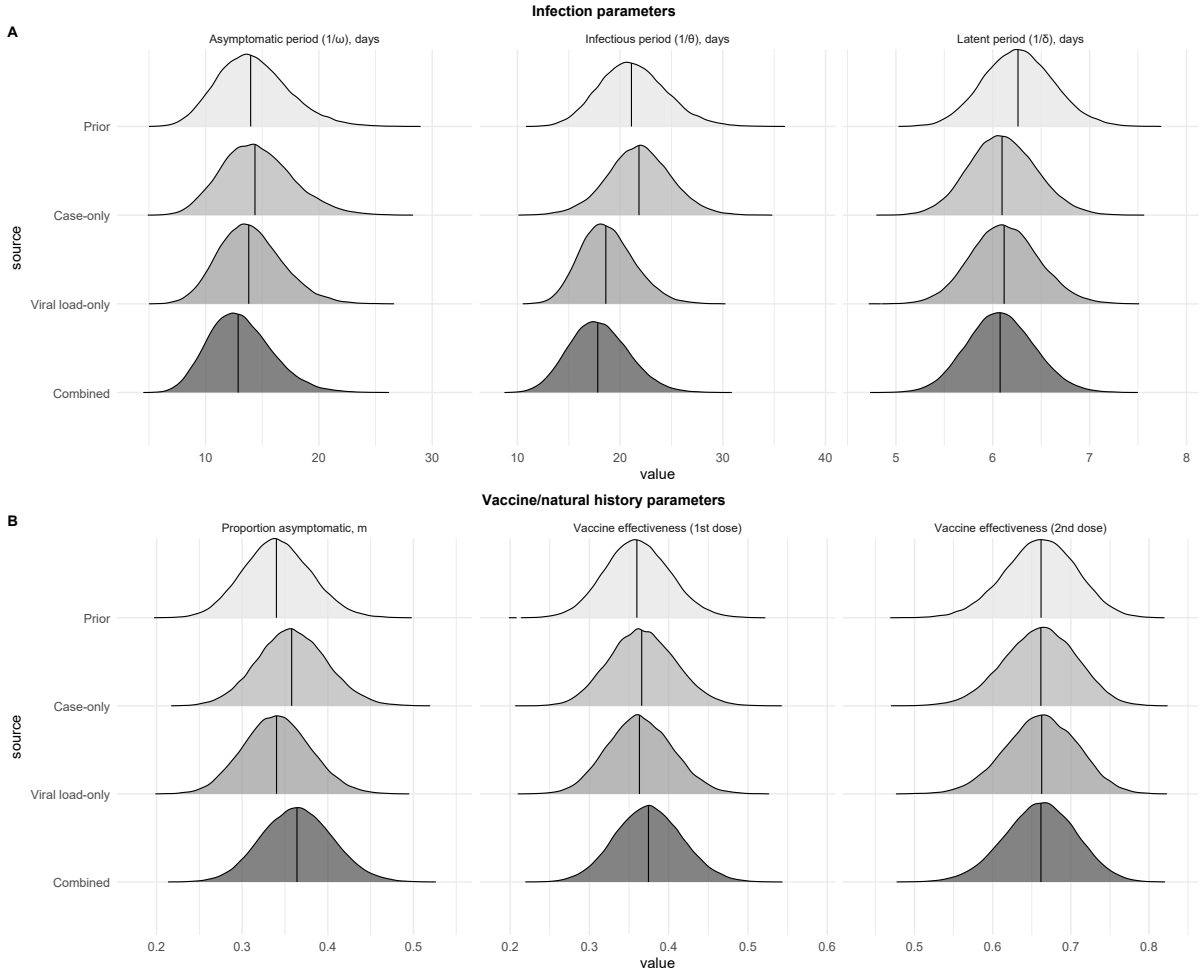

Figure S3: Posterior and prior distributions of key infection, vaccination, and natural history parameters across case-only, wastewater-only, and combined models

References

[1] F. Xiu, C. M. Doyle, J. L. F. Anato, J. Knight, L. Wang, J. Cox, D. Grace, T. A. Hart, T. Zhang, S. Skakoon-Sparling, *et al.*, "Impact of interventions on mpox transmission during the 2022 outbreak in canada: a mathematical modeling study of three different cities," *International Journal of Infectious Diseases*, vol. 153, p. 107792, 2025.

[2] S. P. C. Brand, M. P. C. Cavallaro, J. Hilton, L. M. G. Rincon, T. House, M. J. Keeling, and J. Nokes, "The role of vaccination and public awareness in medium-term forecasts of monkeypox incidence in the United Kingdom," Aug. 2022. ISSN: 2227-8788 Pages: 2022.08.15.22278788.

[3] C. Suñer, M. Ubals, E. J. Tarín-Vicente, A. Mendoza, A. Alemany, Á. Hernández-Rodríguez, C. Casañ, V. Descalzo, D. Ouchi, A. Marc, *et al.*, "Viral dynamics in patients with monkeypox infection: a prospective cohort study in spain," *The Lancet Infectious Diseases*, vol. 23, no. 4, pp. 445–453, 2023.

[4] M. Lajeunesse, "Juicr: automated and manual extraction of numerical data from scientific images," *See https://CRAN. R-project. org/package= juicr (accessed 27 February 2023)*, 2021.

[5] S. Nourbakhsh, A. Fazil, M. Li, C. S. Mangat, S. W. Peterson, J. Daigle, S. Langner, J. Shurgold, P. D'Aoust, R. Delatolla, E. Mercier, X. Pang, B. E. Lee, R. Stuart, S. Wijayasri, and D. Champredon, "A wastewater-based epidemic model for SARS-CoV-2 with application to three Canadian cities," *Epidemics*, vol. 39, p. 100560, June 2022.

[6] J. R. Phaneuf, G. Cha, J. K. Hatt, K. T. Konstantinidis, and K. E. Graham, "Decay and solid-liquid partitioning of mpox and vaccinia virus dna in primary influent and settled solids to guide wastewater-based epidemiology practices," *Water Research*, p. 123904, 2025.

[7] P. Satapathy, P. Mohanty, S. Manna, M. A. Shamim, P. P. Rao, A. K. Aggarwal, J. Khubchandani, A. Mohanty, B. Nowrouzi-Kia, V. K. Chattu, *et al.*, "Potentially asymptomatic infection of monkeypox virus: a systematic review and meta-analysis," *Vaccines*, vol. 10, no. 12, p. 2083, 2022.

[8] N. P. Deputy, J. Deckert, A. N. Chard, N. Sandberg, D. L. Moulia, E. Barkley, A. F. Dalton, C. Sweet, A. C. Cohn, D. R. Little, *et al.*, "Vaccine effectiveness of jynneos against mpox disease in the united states," *New England Journal of Medicine*, vol. 388, no. 26, pp. 2434–2443, 2023.